

DTP/95/40  
ILL-(TH)-95-30  
hep-ph/9505433

May 1995

## Single-top-quark production via $q\bar{q} \rightarrow t\bar{b}$

**T. Stelzer**

Department of Physics  
University of Durham  
Durham DH1 3LE  
England

**S. Willenbrock**

Department of Physics  
University of Illinois  
1110 West Green Street  
Urbana, IL 61801

### Abstract

We consider single-top-quark production via the weak process  $q\bar{q} \rightarrow t\bar{b}$  at hadron colliders. This process may provide the best measurement of the magnitude of the Cabbibo-Kobayashi-Maskawa matrix element  $V_{tb}$ . We show that a signal can potentially be observed at the Fermilab Tevatron with  $3 \text{ fb}^{-1}$  of integrated luminosity. In contrast, the signal is masked at the CERN Large Hadron Collider by top-quark pair production and single-top-quark production via  $W$ -gluon fusion.

# 1 Introduction

The recent discovery of the top quark by the CDF and D0 Collaborations at the Fermi-lab Tevatron has stimulated interest in top-quark physics [1]. The standard model of the strong and electroweak interactions predicts that the top quark should behave, both in its production and decay, as a heavy version of the five lighter quarks. However, the large mass of the top quark relative to the five lighter quarks suggests that there may be something special about its properties. It is therefore crucial that we study the properties of the top quark with every probe available to us.

In this paper we study a neglected probe of the top quark: the process  $q\bar{q} \rightarrow t\bar{b}$  via a virtual  $s$ -channel  $W$  boson, as depicted in Fig. 1(a) [2]. This process is similar to the well-known  $W$ -gluon fusion process [3, 4, 5, 6], depicted in Fig. 1(b), in that it produces a single top quark rather than a  $t\bar{t}$  pair. However, the process  $q\bar{q} \rightarrow t\bar{b}$  probes the top quark with a timelike  $W$  boson,  $q^2 > (m_t + m_b)^2$ , while the  $W$ -gluon-fusion process involves a spacelike  $W$  boson,  $q^2 < 0$ . These processes are therefore complementary in that they probe the charged-current interaction of the top quark in different regions of  $q^2$ .<sup>1</sup>

Another important feature of  $q\bar{q} \rightarrow t\bar{b}$  is that the hadronic cross section can be reliably calculated. The quark and antiquark distribution functions are evaluated at moderate values of  $x$ , where they are well-known. The QCD correction to this process is straightforward and can be carried out to at least  $\mathcal{O}(\alpha_s^2)$ . Furthermore, the initial quark-antiquark flux can be constrained by measuring  $q\bar{q} \rightarrow \bar{\ell}\nu$ , which also proceeds via a virtual  $s$ -channel  $W$  boson.<sup>2</sup> The QCD correction to the initial state is automatically taken into account via this procedure; only the QCD correction to the final state must be explicitly calculated, and this can be done reliably since it is free of collinear and infrared singularities.<sup>3</sup> In contrast, the  $W$ -gluon-fusion process involves the gluon distribution function, which is not well-known.

---

<sup>1</sup>The decay of the top quark,  $t \rightarrow Wb$ , involves an on-shell  $W$  boson,  $q^2 = M_W^2$ .

<sup>2</sup>Since the neutrino longitudinal momentum cannot be reconstructed, the  $q^2$  of the  $W$  boson cannot be determined. The process  $q\bar{q} \rightarrow \bar{\ell}\nu$  therefore provides a constraint on the quark-antiquark flux, not a direct measurement.

<sup>3</sup>The QCD correction to the initial and final states do not interfere until  $\mathcal{O}(\alpha_s^2)$ .

Since the most important issue to be resolved is the observability of  $q\bar{q} \rightarrow t\bar{b}$  above backgrounds, we concentrate on this process in the context of the standard electroweak model. In this context,  $q\bar{q} \rightarrow t\bar{b}$  may provide the best direct measurement of the magnitude of the Cabbibo-Kobayashi-Maskawa (CKM) matrix element  $V_{tb}$ . If there are only three generations, unitarity of the CKM matrix implies that  $|V_{tb}|$  is very close to unity ( $|V_{tb}| = .9988 - .9995$  [7]). If there is a fourth generation,  $|V_{tb}|$  could be anywhere between (almost) zero and unity, depending on the amount of mixing between the third and fourth generations. A measurement of  $|V_{tb}|$  less than unity would therefore be a major discovery.

## 2 Signal and Backgrounds

Including the top-quark decay, the process  $q\bar{q} \rightarrow t\bar{b}$  yields the final state  $Wb\bar{b}$ . There are several background processes which must be considered in order to establish whether the signal can be observed. The dominant irreducible background,  $q\bar{q} \rightarrow Wb\bar{b}$ , was considered in Ref. [2]. We reconsider this background, as well as the other important irreducible and reducible backgrounds. The full set of backgrounds we consider is:

- $Wb\bar{b}$
- $Wjj$  (where  $j$  denotes a light-quark or gluon jet)
- $WZ \rightarrow Wb\bar{b}$
- $qg \rightarrow t\bar{b}j \rightarrow Wb\bar{b}j$  ( $W$ -gluon fusion)
- $t\bar{t} \rightarrow W^+W^-b\bar{b}$

The raw cross sections for these processes at the Tevatron ( $\sqrt{s} = 2$  TeV  $p\bar{p}$  collider) and the CERN Large Hadron Collider (LHC,  $\sqrt{s} = 14$  TeV  $pp$  collider) are given in the first column of Table 1. We use  $m_t = 175$  GeV, and all cross sections are calculated at leading order.<sup>4</sup>

---

<sup>4</sup>The helicity amplitudes for the processes in this paper are generated by MadGraph [8]. We use the MRS(A') parton distribution functions [9], evaluated at  $\mu^2 = \hat{s}$ , for all cross sections except  $W$ -gluon fusion, where we use  $\mu^2 = M_W^2$ . We evaluate  $\alpha_s(\mu)$  at the same scale as the parton distribution functions, with  $\alpha_s(M_Z) = .117$  [7].

The cross sections include a factor of  $2/9$  for the branching ratio of  $W \rightarrow \bar{\ell}\nu$  ( $\ell = e, \mu$ ). The cross sections listed are for  $W^+$  production only; the inclusion of  $W^-$  doubles the signals and backgrounds at the Tevatron, and nearly doubles them at the LHC. The  $Wjj$  cross section is infinite without cuts due to infrared and collinear singularities.

We smear the jet energies with a Gaussian function of width  $\Delta E_j/E_j = 0.80/\sqrt{E_j} \oplus 0.05$  (added in quadrature) to simulate the resolution of the hadron calorimeter. We do not smear the lepton energy, since this is a small effect compared with the smearing of the jet energies. We show in Fig. 2 the transverse-momentum spectra of the  $b$  jet, the  $\bar{b}$  jet, and the lepton for the signal process. We list in Table 2 the cuts imposed on the signal and backgrounds to simulate the acceptance of the detector. The resulting cross sections are listed in the second column of Table 1. The acceptance for the signal is 50% at the Tevatron and 25% at the LHC.<sup>5</sup>

In the third column of Table 1, the  $W$ -gluon fusion background (denoted by  $t\bar{b}j$ ) is reduced by rejecting events in which a third jet is detected with  $p_{Tj} > 20$  GeV and  $|\eta_j| < 4$ . This provides a reduction factor of about  $1/5$  at both the Tevatron and the LHC. This also reduces the signal cross section, since the signal will sometimes be accompanied by a third jet due to QCD radiation. We estimate<sup>6</sup> this reduction to be about 15% at the Tevatron and about 35% at the LHC, and reduce the signal accordingly.<sup>7</sup> The  $Wb\bar{b}$ ,  $Wjj$ , and  $WZ$  backgrounds would also be reduced; but, to be conservative, we have not taken this into account.

The  $t\bar{t}$  background is reduced by rejecting events with an additional  $W$  boson. If the  $W$  boson decays hadronically, the event is rejected if either jet has  $p_{Tj} > 20$  GeV and  $|\eta_j| < 4$ . If the  $W$  boson decays leptonically,<sup>8</sup> the event is rejected if  $p_{T\ell} > 10$  GeV and  $|\eta_\ell| < 2.5$ .

---

<sup>5</sup>The acceptance at the LHC will actually be larger since the vertex detector extends to  $|\eta_b| < 2.5$  [10, 11].

<sup>6</sup>This estimate is derived from a calculation of  $t\bar{b}$  plus an additional jet, and an estimate of the QCD correction to the inclusive cross section based on the correction to  $q\bar{q} \rightarrow \bar{\ell}\nu$ .

<sup>7</sup>Since  $W$ -gluon fusion is a small background at the Tevatron, it may be advantageous to increase the jet-rejection threshold in order to preserve more of the signal. With a threshold of  $p_{Tj} > 30$  GeV, we estimate that almost none of the signal is lost, while the small  $W$ -gluon fusion background is increased by only a factor of 1.8.

<sup>8</sup>We treat the  $\tau$  similar to  $e, \mu$  for this  $W$  decay. This may underestimate the background for  $W \rightarrow \bar{\tau}\nu$ .

The overall reduction factor from rejecting these events is  $1/50$  at the Tevatron and  $1/30$  at the LHC. Most of the remaining background events are from the leptonic decay of the extra  $W$  boson (75% at the Tevatron, 85% at the LHC).<sup>9</sup>

In the fourth column of Table 1, we impose a cut on the  $b\bar{b}$  invariant mass,  $M_{b\bar{b}} > 110$  GeV. This essentially eliminates the  $WZ \rightarrow Wb\bar{b}$  background, and reduces the  $Wb\bar{b}$  and  $Wjj$  backgrounds. The loss of signal is modest.<sup>10</sup> If there is a Higgs boson of mass less than 120 GeV, it too will contribute to the background via  $WH \rightarrow Wb\bar{b}$  [12, 13, 14], and may require a slightly higher cut on  $M_{b\bar{b}}$ .

Due to the enormous background from  $Wjj$  (where  $j$  denotes a jet from a light quark or gluon), it is necessary to tag one or both of the  $b$  quarks from the  $q\bar{q} \rightarrow t\bar{b} \rightarrow Wb\bar{b}$  signal. The most efficient means of  $b$  tagging is with a silicon vertex detector (SVX). The CDF Collaboration has achieved a tagging efficiency of roughly 40% per “fiducial”  $b$  jet ( $p_{Tb} > 20$  GeV and within the coverage of the SVX), with a probability of less than 1% for a light-quark or gluon jet to fake a  $b$  jet [15]. The new SVX for Run II, with three-dimensional vertex information, should increase the efficiency to as high as 60% while maintaining or reducing the fake rate [16]. Pixel detectors, such as those planned for the ATLAS [10] and CMS [11] detectors at the LHC, could further increase the efficiency. We assume a 60% tagging efficiency<sup>11</sup> per fiducial  $b$  jet ( $p_{Tb} > 20$  GeV,  $|\eta_b| < 2$ ) with a 1% fake rate from fiducial light-quark and gluon jets. The best signal significance is obtained by tagging both  $b$  jets.<sup>12</sup>

The final column in Table 1 lists the cross sections including the  $b$ -tagging efficiency. With double  $b$  tagging, the  $Wjj$  background is reduced to a negligible level at the Tevatron.

Another piece of information at our disposal is the invariant mass of the  $W$  boson plus  $b$  jet,  $M_{Wb}$ , which equals  $m_t$  for the signal but has a continuous spectrum for the  $Wb\bar{b}$  background. Unfortunately, this information cannot be utilized directly. One does not know

---

<sup>9</sup>The threshold for rejecting leptons could potentially be lowered below  $p_{T\ell} > 10$  GeV. This is unnecessary at the Tevatron, but is desirable at the LHC, where  $t\bar{t}$  is the largest background.

<sup>10</sup>It may be advantageous to relax this cut to preserve more of the signal.

<sup>11</sup>The soft-lepton tag also contributes a small amount to the  $b$ -tagging efficiency.

<sup>12</sup>With single  $b$  tagging, the  $W$ -gluon-fusion background is prohibitively large. The  $\bar{b}$  jet is often below the  $p_T > 20$  GeV threshold, and the  $b$  jet from the top decay plus the spectator jet (from the radiation of the virtual  $W$ ) fake the signal.

*a priori* which  $b$  jet is from the top-quark decay. Furthermore, the  $W$ -boson momentum must be reconstructed from the lepton momentum plus the missing  $p_T$ , and this yields two solutions. Thus each event has four possible assignments of momenta, leading to four different values of  $M_{Wb}$ .

The most straightforward method to deal with this four-fold ambiguity is to assign four values of  $M_{Wb}$  to each event, and plot the differential cross section as a function of this invariant mass (weighting each entry by 1/4 of an event). The resulting invariant-mass distributions for the signal and the largest backgrounds are shown in Fig. 3(a) at the Tevatron and Fig. 3(b) at the LHC. The signal is prominent at the Tevatron, but is masked by the  $t\bar{t}$  and  $W$ -gluon-fusion backgrounds at the LHC, which have the same shape as the signal. These backgrounds are enhanced at the LHC relative to the  $q\bar{q} \rightarrow t\bar{b}$  signal because they are initiated by gluons.

In  $p\bar{p}$  collisions, the  $b$  jet from the process  $q\bar{q} \rightarrow t\bar{b} \rightarrow Wb\bar{b}$  tends to go in the direction of the proton beam [2]. This can be used to select the correct  $b$  jet to associate with the  $W$  boson, with an efficiency of about 80%. Furthermore, the correct neutrino solution tends to be the one with the smaller absolute longitudinal momentum. Making these assignments, we show in Fig. 4 the resulting invariant-mass distribution at the Tevatron. The signal is significantly narrower than in Fig. 3(a), and clearly stands out above the  $Wb\bar{b}$  and  $t\bar{t}$  backgrounds.

Selecting a bin of width 40 GeV centered on 175 GeV in Fig. 4, the signal cross section is 4.4  $fb$  and the background 3.4  $fb$ . Including the charge-conjugate process,  $q\bar{q} \rightarrow \bar{t}b$ , the total signal is 8.8  $fb$  on a background of 7.2  $fb$ . The number of events acquired in 3  $fb^{-1}$  of integrated luminosity is enough for the signal to correspond to more than a  $5\sigma$  fluctuation of the continuum background. This integrated luminosity corresponds to about 1.5 years of running at the Tevatron with the Main Injector and the Recycler ( $\mathcal{L} = 2 \times 10^{32}/cm^2/s$ ) [17].

Assuming  $|V_{tb}|$  is close to unity, 3  $fb^{-1}$  of integrated luminosity yields a 10% measurement of  $|V_{tb}|$ . This corresponds to a 20% measurement of the partial width  $\Gamma(t \rightarrow Wb)$ . A 5% measurement of  $|V_{tb}|$  requires 12  $fb^{-1}$ , which could be delivered in a little more than a

year with a high-luminosity Tevatron ( $\mathcal{L} = 10^{33}/\text{cm}^2/\text{s}$ ) [17]. This corresponds to a 10% measurement of  $\Gamma(t \rightarrow Wb)$ . The systematic error in the measurement is small, as discussed in the Introduction.

If  $|V_{tb}|$  is significantly less than unity, the rate for  $q\bar{q} \rightarrow t\bar{b}$  is suppressed, and this process is therefore more difficult to detect. If no signal is observed with  $3 \text{ fb}^{-1}$  of integrated luminosity, an upper bound of  $|V_{tb}| < 0.60$  (95% C. L.) can be deduced. The absence of a signal with  $12 \text{ fb}^{-1}$  implies  $|V_{tb}| < 0.40$ .

### 3 Conclusions

We have shown that the process  $q\bar{q} \rightarrow t\bar{b}$  is potentially observable at the Tevatron with  $3 \text{ fb}^{-1}$  of integrated luminosity. The signal is straightforward to isolate from backgrounds, and requires tagging both  $b$  jets. In contrast, this process is masked at the LHC by backgrounds from  $t\bar{t}$  and single-top-quark production via  $W$ -gluon fusion. We hope this work will motivate a more detailed study of this process by the detector collaborations.

The process  $q\bar{q} \rightarrow t\bar{b}$  at the Tevatron may be the best direct measurement of  $|V_{tb}|$ . The  $W$ -gluon fusion process also provides a measurement of  $|V_{tb}|$  [4], and has the advantage of a larger cross section. However, it suffers from the uncertainty in the gluon distribution function. In contrast, the quark-antiquark flux for  $q\bar{q} \rightarrow t\bar{b}$  is well-known, and can be constrained by measuring  $q\bar{q} \rightarrow \bar{\ell}\nu$ . Both  $q\bar{q} \rightarrow t\bar{b}$  and  $W$ -gluon fusion should be pursued, since they probe the top-quark charged current in different regions of  $q^2$ .

### Acknowledgements

We are grateful for conversations with C. Hill, S. Parke, and T. Liss. T. S. was supported in part by a UK PPARC Post-Doctoral Fellowship. S. W. was supported in part by Department of Energy grant DE-FG02-91ER40677.

### References

- [1] CDF Collaboration, F. Abe *et al.*, Phys. Rev. Lett. **74**, 2626 (1995); D0 Collaboration, S. Abachi *et al.*, Phys. Rev. Lett. **74**, 2632 (1995).
- [2] S. Cortese and R. Petronzio, Phys. Lett. **B253**, 494 (1991).
- [3] S. Willenbrock and D. Dicus, Phys. Rev. D **34**, 155 (1986).
- [4] C.-P. Yuan, Phys. Rev. D **41**, 42 (1990); D. Carlson and C.-P. Yuan, Phys. Lett. **B306**, 386 (1993).
- [5] R. K. Ellis and S. Parke, Phys. Rev. D **46**, 3785 (1992).
- [6] G. Bordes and B. van Eijk, Nucl. Phys. **B435**, 23 (1995).
- [7] *Review of Particle Properties*, Phys. Rev. D **50**, 1173 (1994).
- [8] T. Stelzer and W. F. Long, Comput. Phys. Commun. **81**, 357 (1994).
- [9] A. Martin, R. Roberts, and W. J. Stirling, RAL-95-021 (1995), to be published in Phys. Lett. B.
- [10] ATLAS Technical Proposal, CERN/LHCC/94-43, LHCC/P2 (1994).
- [11] CMS Technical Proposal, CERN/LHCC/94-38, LHCC/P1 (1994).
- [12] A. Stange, W. Marciano, and S. Willenbrock, Phys. Rev. D **49**, 1354 (1994); D **50**, 4491 (1994).
- [13] D. Froidevaux and E. Richter-Was, CERN-TH-7459-94 (1994).
- [14] S. Mrenna and G. Kane, CALT-68-1938 (1994).
- [15] T. Liss, private communication.
- [16] D. Amidei, private communication.
- [17] W. Foster, private communication.



Table 1: Cross sections ( $fb$ ) for  $q\bar{q} \rightarrow t\bar{b}$  and a variety of background processes at the Tevatron and the LHC. The cross sections should be multiplied by a factor of two at the Tevatron, and nearly a factor of two at the LHC, to include  $q\bar{q} \rightarrow \bar{t}b$ . The  $W$ -gluon-fusion background is denoted by  $\bar{t}bj$ . The first column is the total cross section times a factor of 2/9 for the branching ratio of the  $W$  boson to  $e, \mu$ . The second column adds the cuts listed in Table 2 to simulate the acceptance of the detector. The third column includes the rejection of events with an additional identified jet or lepton. The fourth column adds a cut on the invariant mass of the  $b\bar{b}$  pair. The final column includes the efficiency for double  $b$  tagging, taken to be 36% per event (based on 60% efficiency per fiducial  $b$  jet). The fake rate for light-quark and gluon jets is taken to be 1% per jet.

	Tevatron		2 TeV $p\bar{p}$		
	Total $\times BR$	Acceptance	Rejection	$M_{b\bar{b}} > 110$ GeV	$b$ tagging
$t\bar{b}$	69	34	29	18	6.5
$Wb\bar{b}$	3250	140	140	25	9.0
$Wjj$	—	14000	14000	3500	0.35
$WZ$	51	22	22	0.71	0.26
$\bar{t}bj$	116	31	5.7	2.3	0.83
$t\bar{t}$	860	505	9.5	6.0	2.2

	LHC		14 TeV $pp$		
	Total $\times BR$	Acceptance	Rejection	$M_{b\bar{b}} > 110$ GeV	$b$ tagging
$t\bar{b}$	1100	290	190	130	47
$Wb\bar{b}$	34500	925	925	235	85
$Wjj$	—	340000	340000	140000	14
$WZ$	785	156	156	6.6	2.4
$\bar{t}bj$	21000	4800	1100	615	220
$t\bar{t}$	90500	40000	1200	810	290

Table 2: Acceptance cuts used to simulate the detector. The  $p_{T\ell}$  threshold is greater for charged leptons which are used as triggers (in parentheses).

$ \eta_b  < 2$	$p_{Tb} > 20 \text{ GeV}$
$ \eta_\ell  < 2.5$	$p_{T\ell} > 10 \text{ GeV (20 GeV)}$
$ \eta_j  < 4$	$p_{Tj} > 20 \text{ GeV}$
$ \Delta R_{b\bar{b}}  > 0.7$	$ \Delta R_{b\ell}  > 0.7$
$\cancel{p}_T > 20 \text{ GeV}$	

## Figure Captions

Fig. 1 - Feynman diagrams for single-top-quark production via (a)  $q\bar{q} \rightarrow t\bar{b}$  via a virtual timelike  $W$  boson, and (b)  $W$ -gluon fusion via a virtual spacelike  $W$  boson.

Fig. 2 - Transverse-momentum spectra of the  $b$ ,  $\bar{b}$ , and lepton from  $q\bar{q} \rightarrow t\bar{b} \rightarrow Wb\bar{b}$ , followed by leptonic decay of the  $W$  boson, at the Tevatron.

Fig. 3 - Differential cross section for  $q\bar{q} \rightarrow t\bar{b} \rightarrow Wb\bar{b}$  versus the invariant mass of the  $W$  boson and  $b$  jet at (a) the Tevatron and (b) the LHC. Also shown are the most important backgrounds ( $t\bar{b}j$  denotes  $W$ -gluon fusion). Each event contributes four points to the distribution, each weighted by  $1/4$ , due to the ambiguity in the  $b$  vs.  $\bar{b}$  and the two-fold ambiguity in the neutrino longitudinal momentum. The signal is prominent at the Tevatron, but is masked by the  $t\bar{t}$  and  $W$ -gluon-fusion backgrounds at the LHC.

Fig. 4 - Same as Fig. 3(a), except the  $b$  jet with the highest rapidity with respect to the proton beam direction is selected as the  $b$  from top decay, and the neutrino solution with the smaller absolute longitudinal momentum is selected. This narrows the distribution from the signal in comparison with Fig. 3(a).

# Diagrams by MadGraph

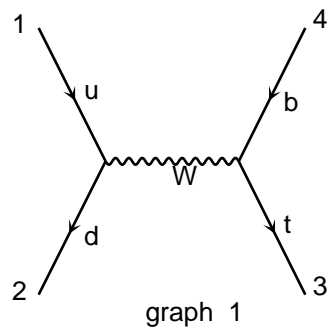


Fig. 1(a)

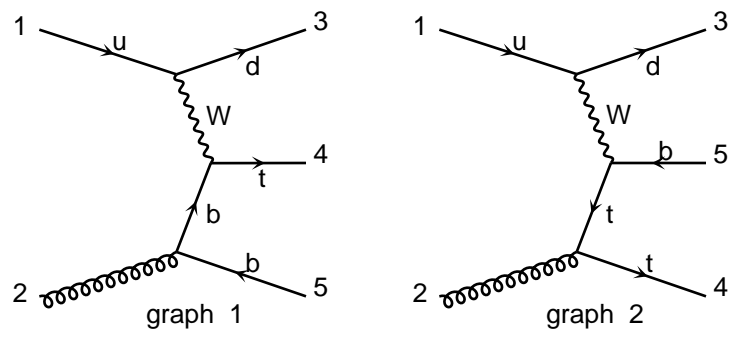


Fig. 1(b)

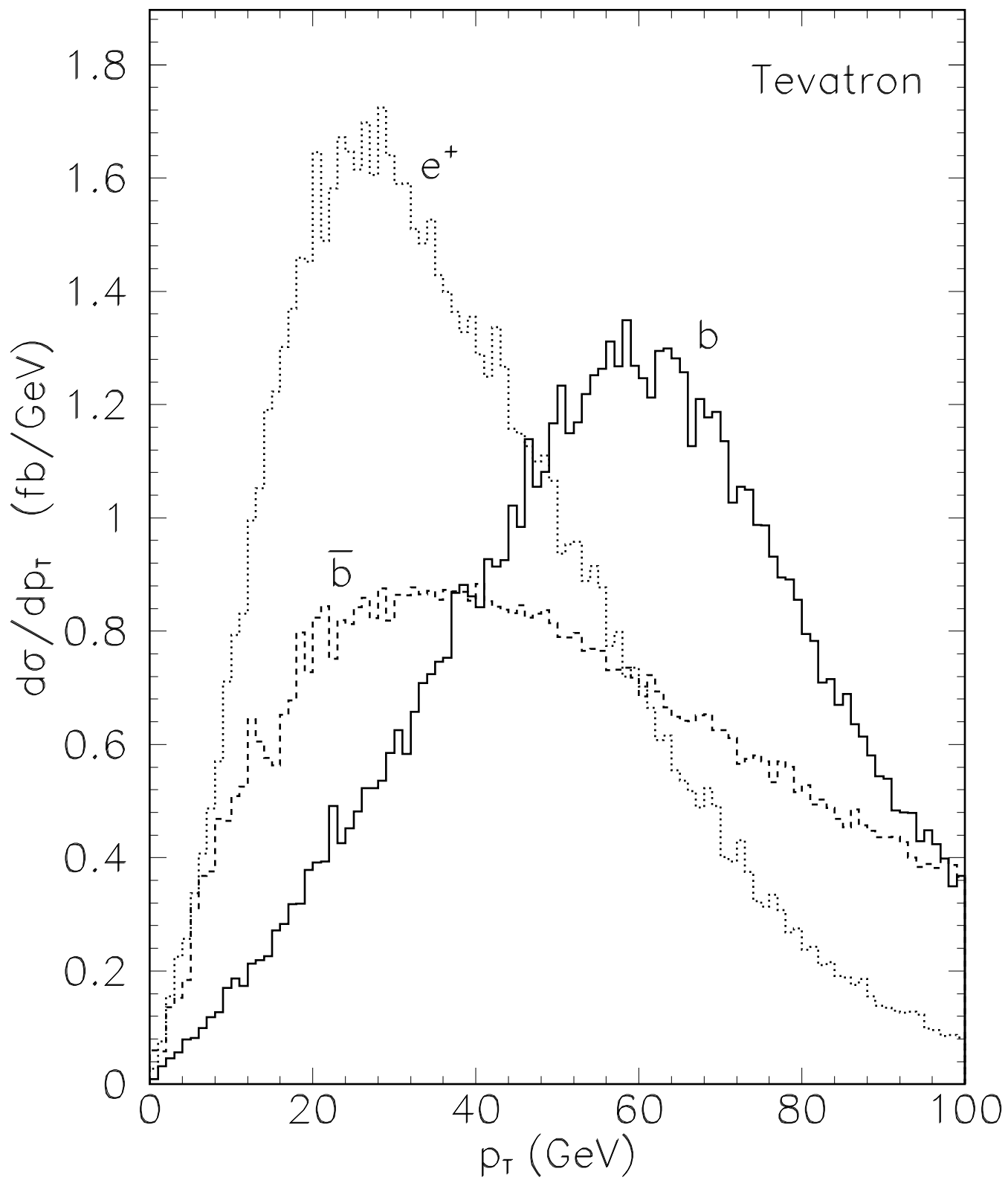


Fig. 2

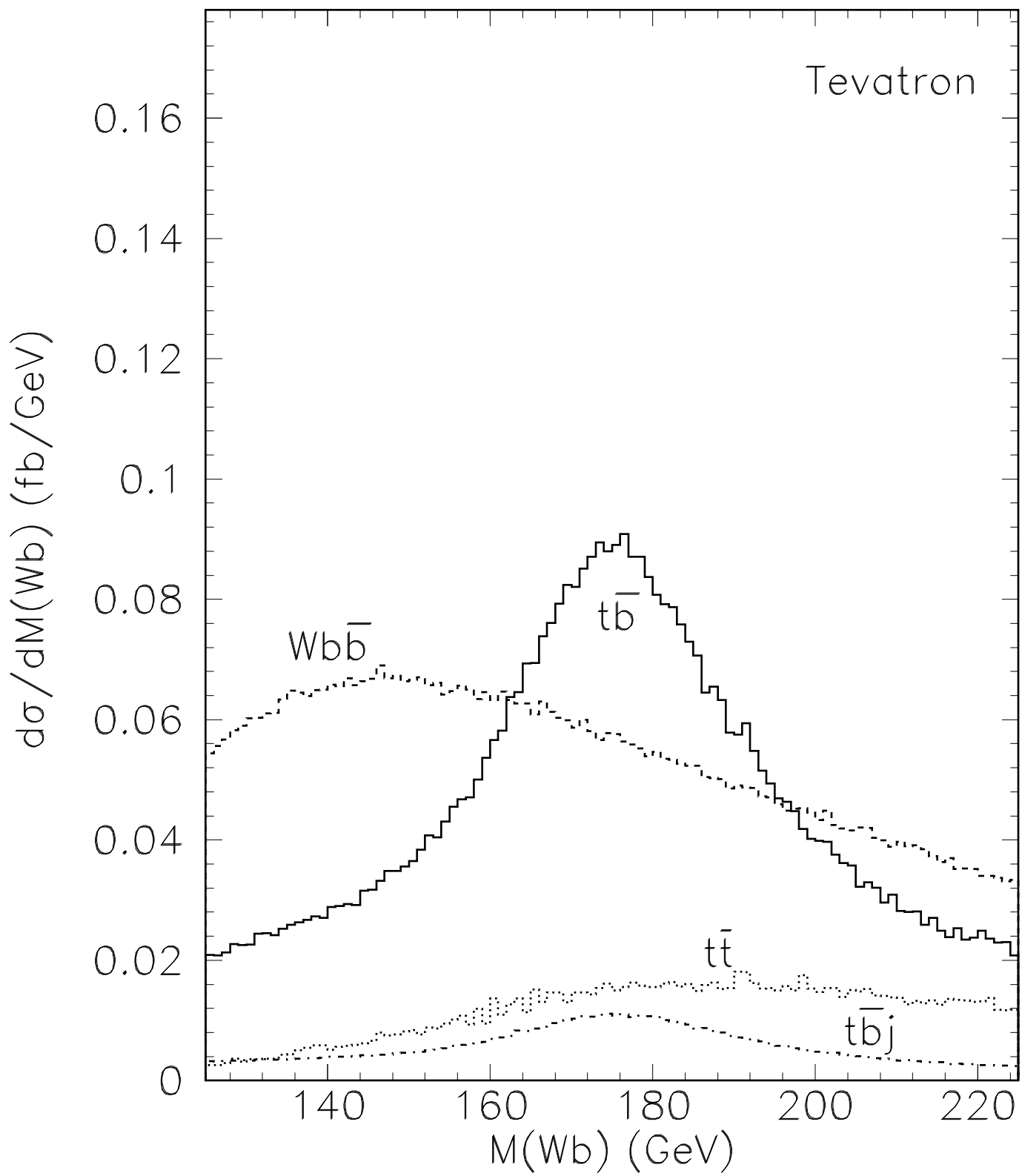


Fig. 3(a)

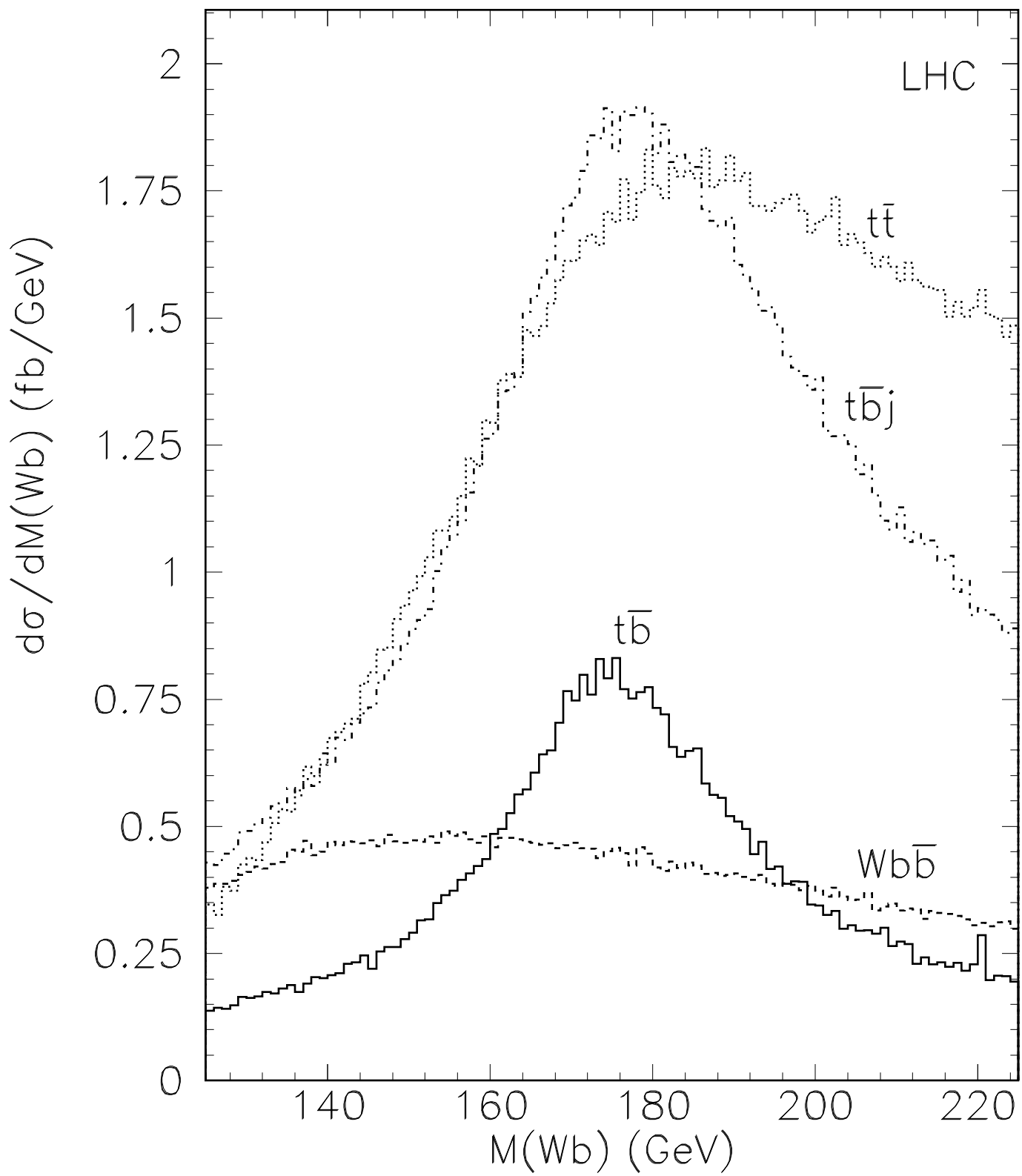


Fig. 3(b)

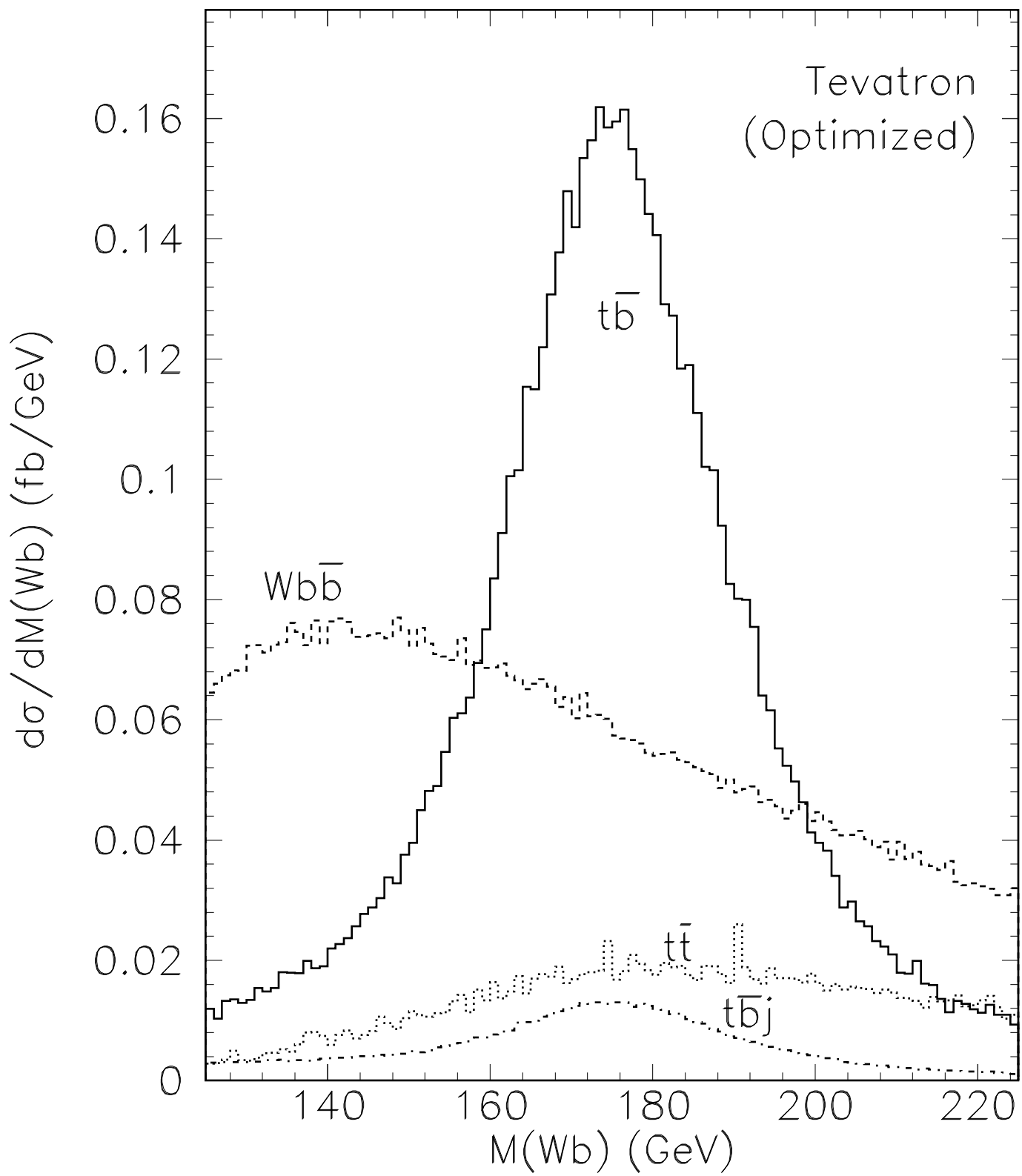


Fig. 4